

Preservation of the protective function of calcium aluminate-based coating against biodeterioration in presence of cracks

Reem Hoballah^{1,2}, Matthieu Peyre Lavigne², Cédric Patapy¹, Laurie Lacarriere¹, Ahmed Toumi¹, Amr Aboulela³, Alexandra Bertron¹

¹Université de Toulouse, UPS, INSA, France

²Université de Toulouse, CNRS, INRA, INSA, TBI, France

³Imerys Technology Center, France

Received: 18 February 2025 / Accepted: 24 October 2025 / Published online: 05 November 2025

© The Author(s) 2025. This article is published with open access and licensed under a Creative Commons Attribution 4.0 International License.

Abstract

The durability of wastewater treatment plants has been a major concern for decades due to their significant economic and health importance. Structures built with concrete are subject to severe deterioration linked to aggressive chemical and biological exposure conditions. Portland cement concrete is particularly vulnerable to such attacks leading to major damages in the structures. One of the strategies to protect this concrete from the effects of biodeterioration is applying a thin coating based on calcium aluminate cement. These materials were proved to have a superior resistance to biodeterioration compared to ordinary Portland cement. However, the cracks initiated in the protected structure that might reach the coating raise questions on its ability to fulfill its protective role. This paper aims to study the effect of the crack on the durability of the coating using a biological laboratory test, the BAC test, which simulates the real conditions encountered in a sewer system. The calcium leached from the specimens exposed to the biogenic sulfuric acid attack was monitored in two campaigns of the BAC test. Each campaign was performed on reference OPC-based uncoated specimens and coated specimens with the CAC-based coating: uncracked and cracked with two ranges of crack width between 150 and 200 μm and between 400 and 500 μm . The leaching results demonstrate that the protective function was not altered by the effect of the cracks when comparing the reference uncoated specimen to the coated ones. The SEM-EDS observations show the existence of a newly-formed phase in the few hundreds of micrometers from the exposed surface of the coated specimens. This phase was composed mainly of calcium, sulfur and aluminum and was probably a mix of AH3 and ettringite. The formation of this phase near and inside the crack opening could possibly act as a physical barrier that prevents further deterioration.

Keywords: Durability test; Wastewater treatment plants; Calcium aluminate cement; Biodeterioration; Cracking.

1 Introduction

One of the 17 goals set by the United Nations for Sustainable Development in 2015 includes water sanitation to ensure its availability and sustainable management for all (SDG6). Implementing this goal extends beyond simply ensuring that water and sanitation services are accessible to all populations; it entails measures that promote the sustainable use and management of water resources [1]. It takes into account the durability of wastewater treatment plants (WWTPs) which must be well-managed to enable a longer service life with reduced operation costs.

The main material used in the construction of different compartments of wastewater treatment plants is concrete. However, the complexity of the wastewater treatment steps and the activity of micro-organisms in wastewater subjects the concrete to aggressive biological and chemical exposure

conditions [2] which ultimately reduce the asset's lifespan. In sewer pipes and manholes for example, sulfate-reducing bacteria produce hydrogen sulfide in the effluent in anaerobic conditions [3,4]. This compound degases and rises to the headspace where sulfur-oxidizing bacteria convert it into sulfuric acid. The concrete is then attacked by the biogenic acid formed [5,6]. Other concrete structures that can also be affected may include primary and secondary sedimentation tanks where sludge accumulates, aeration tanks, clarifiers, and digesters.

Microbially-induced concrete deterioration (MICD) can induce significant structural failure in wastewater treatment plants if not properly managed. The sulfuric acid produced in the process attacks the cementitious matrix leading to strong decalcification of the cement matrix, and the formation of ettringite or gypsum. These expansive compounds induce an increased internal pressure leading to the formation of cracks

*Corresponding author: Reem Hoballah, E-mail: hoballah@insa-toulouse.fr

and spalling of concrete [7,8] and thus the possible loss of the structure's mechanical strength. Moreover, the cracks can provide preferential paths for further acid penetration and concrete deterioration including pH reduction which leads to the proliferation of sulfur-oxidizing bacteria.

Different methods and techniques are used worldwide nowadays to protect concrete wastewater treatment plants. One way to mitigate the effects of MICD is to apply different types of coatings more resistant to biodeterioration than the supporting concrete. Cementitious coatings are widely used due to their chemical compatibility with the concrete used in construction and their improved resistance to biogenic acid deterioration compared to conventional Portland cement concrete. Polymeric coatings, such as epoxies, polyurethanes, polyurea and vinyl ester resins, provide dense and impermeable barriers with strong chemical resistance. However, these coatings lack durability and too often fail after only a few years. Hybrid systems, including polymer-modified mortars and epoxy–cement composites, are also applied aiming to combine the adhesion and chemical stability of mineral phases with the impermeability and flexibility of polymers.

It was widely established in the literature that calcium aluminate cement-based materials have a superior performance of in resisting biodeterioration compared to ordinary Portland cement-based (OPC) materials [9–11]. A cementitious coating was developed for the protection of concrete wastewater treatment plants. This coating is based on calcium aluminate cement (CAC) and a reactive granular phase of the Alag® type. It is spray-applied to newly-built wastewater treatment structures in small thickness or in greater thickness for rehabilitation and protection of existing wastewater infrastructure. Although the product is originally estimated to provide a service life of 30 years, asset owners rehabilitated with a similar type of CAC-based coating have reported expected service life of 50 to 100 years.

Early-age evolutions in the structure and its different movements throughout its service life might initiate cracks which can propagate into the surface of the coating. These cracks may act as preferential routes for the penetration of aggressive agents into the protected concrete. The acid produced on the exposed surface might penetrate through the crack to the substrate, and so do the microorganisms, which can then produce aggressive metabolites close to the substrate [12,13] possibly altering the protective function of the coating. Although the improved performance of this coating was demonstrated in several in-situ tests and laboratory testing methods, the effect of presence of cracks on its protective function was never studied in the literature.

This paper aims to evaluate whether the coating fulfils its protective function for the concrete substrate when exposed to the biogenic acid attack with the presence of cracks. Specimens were exposed to a biological test, the Biogenic Acid Concrete (BAC) test, which simulates the real exposure conditions encountered in a sewer network. The outcome of two campaigns of the BAC test were summarized where an OPC-based specimen was compared to specimens coated with the CAC-based coating; one uncracked specimen and

two cracked specimens. The three-point bending test was performed to obtain the cracked composite specimens with different ranges of crack width: between 150 and 200 µm and between 400 and 500 µm. The investigation was carried out based on the quantification of calcium leaching and the SEM-EDS observations and analyses of microstructural and chemical changes in the deteriorated zones.

2 Materials and methods

Composite specimens composed of a fiber-reinforced mortar substrate coated with a sprayed coating were prepared, cured and then cracked. This procedure was explained in details in our previous publication [14]. The main steps are reminded here.

2.1 Materials for substrate and coating

The substrate blocks were cast with fiber-reinforced mortar with CEM III/A 42.5 N-LH according to FD P 18-011 [15] standard in the case of severe chemical attack in an acidic environment (XA3). To improve the cracking capacity of these samples and, above all, to be able to produce cracks with controlled opening, FibraFlex® amorphous metallic fibers were introduced into the substrate formulation presented in Table 1. These fibers are 20 mm in length with a width of 1.6 mm and a thickness of 29 µm. In fact, plain concrete could not sustain crack openings wider than 150 µm before sudden and complete failure occurred. The fiber reinforcement was therefore necessary to stabilize the crack propagation and to allow the investigation of wider, controlled crack openings that would otherwise not be achievable with plain concrete.

Table 1. Mix proportions of the fiber-reinforced mortar used in the substrate formulation.

Component	Quantity / m ³
Cement (CEM III/A 42,5 N-LH)	500 kg
Sand (maximum particle size 4 mm)	1606 kg
Water	235 kg
Superplasticizer (Sika® ViscoCrete® Tempo-413)	1,25 ml
Fibraflex amorphous metal fibers	20 kg

2.2 Preparation of composite specimens

Over two experimental campaigns, the formulation presented in Table 1 was used to cast the substrates into 7 cm x 7 cm x 28 cm molds followed by the same wet-curing protocol in water for 14 days. These mortar blocks were then placed in sealed bags with controlled conditions of 20°C with 50% RH for 70 days in the first campaign and 14 days in the second. The curing time duration was reduced between the two campaigns to improve time efficiency. The specimens were covered at both ends before spraying to ensure the finishing of the surface is flat and thus compatible with the cracking procedure.

The calcium aluminate cement-based coating was then spray-applied onto the OPC-based substrate blocks with a thickness of 5 mm as shown in Figure 1. This coating was based on calcium aluminate cement and a reactive granular phase of the Alag® type which is a synthetic non-hydrated calcium

aluminate aggregate. It is manufactured by the fusion of limestone and bauxite into a crushed and sized aggregate of approximately 40% alumina. The substrate-coating composite specimens were then left to dry in the ambient conditions of the lab for 7 days.

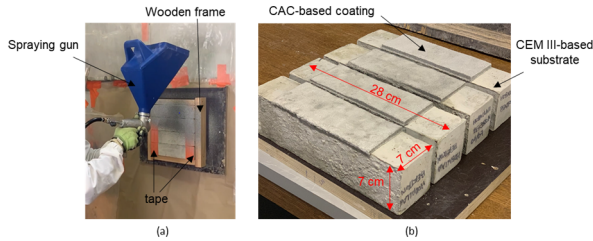


Figure 1. (a) Photo showing procedure of spraying the coating using the spraying gun on the substrates placed in the wooden frame with their edges covered with tape; (b) the prepared coating-substrate specimens.

2.3 Crack generation procedure

To initiate cracks in the prepared substrate-coating composite specimens, three-point bending test was performed with the setup in Figure 2. These tests were conducted using the Materials Test Systems (MTS) press, a model from the Landmark® Servo Hydraulic Test Systems featuring a 10-ton pressure gauge whose setup is shown in Figure 2.

The application of the load was controlled with the rate of increase of displacement control measured with the assistance of a linear variable differential transformer (LVDT) with 1 mm precision. The rate of displacement was set at 5 μm/min until the peak load was reached after which the displacement rate increased to 10 μm/min as the load progressively decreased. To monitor the crack opening during loading, a hand-held Dino-Lite Edge Digital USB video-microscope was used.

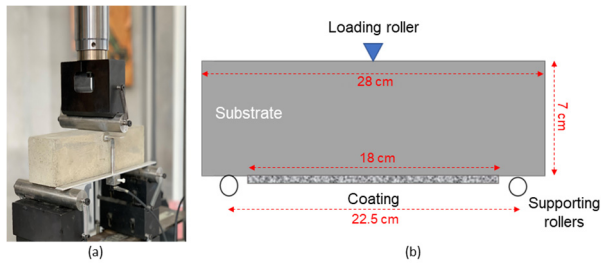


Figure 2. The setup of the 3-point bending test for the cracking procedure in (a) a photo and (b) a scheme.

To study the effect of the crack on the protective function of the coating, two ranges of width of the surface crack opening were studied. The first crack ranging between 150 and 200 μm was considered the narrow crack, which falls below the limiting value of crack width in Eurocode 2 [16]. The second crack ranging between 400 and 500 μm was considered the wide crack. These crack widths were measured after unloading and monitored for several weeks to ensure that the crack opening maintains its surface width without re-closure.

2.4 Preparation of specimens for BAC test

The cracked composite specimens were sawn as shown in Figure 3 to obtain the specimens to be exposed to biodeterioration in laboratory conditions.

The unexposed surfaces of the cementitious specimens were covered with an epoxy resin, EUROKOTE 48-20, leaving only the top surface exposed to the biogenic acid attack as shown in Figure 3. Thin lines of resin were also applied to the edges of the exposed surface to drive the feeding solution to flow from upstream of the specimen to downstream.

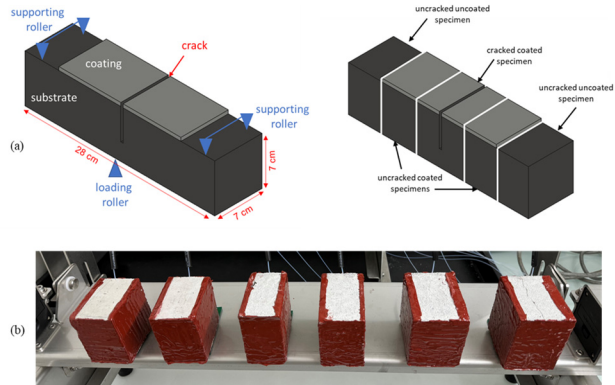


Figure 3. (a) A scheme showing the preparation of specimens by sawing of cracked composite specimen (b) a photo showing the unexposed surfaces of specimens covered with epoxy resin to be exposed to the BAC test.

2.5 Biological test: BAC test

To assess the performance of the composite specimens when subject to biodeterioration, they were exposed to the conditions encountered in sewer networks simulated in the Biogenic Acid Concrete (BAC) test: a biological test developed at INSA Toulouse [11,17]. It uses the inoculation of a biofilm on the surface of the material under study, fed by dripping a reduced sulfur source of tetrathionate solution over it.

The test apparatus shown in Figure 4 consists of a support on which the specimens are fixed. The support is slightly inclined to enable the feeding solution to flow over the exposed surface. The top surface of each specimen is inoculated with activated sludge. A 200-liter tanks is filled with the feeding solution consisting of a soluble reduced sulfur source, tetrathionate ($K_2S_4O_6$) [18], with other nutrients dissolved in deionized water for the development of microorganisms. This feeding solution in the tank is then transported through plastic tubes and a pump to drip on the upstream of the exposed surfaces and flow to the downstream where it gets collected frequently to analyze the leached species.

The duration of the specimens' exposure to the BAC test is usually 3 months. The first experimental campaign was interrupted at 67 days because of a technical problem. The second experimental was then launched with a proper exposure period of 3 months and minor modifications in the preparation of the specimens to improve the conditions of the test. The different types of cementitious materials that were exposed are a non-coated mortar substrate (CEM III), a coated cracked mortar substrate, and a coated non-cracked mortar substrate. The biodeterioration process was

monitored throughout the exposure period through analyzing the composition of the leached solutions and microstructural and chemical analyses.

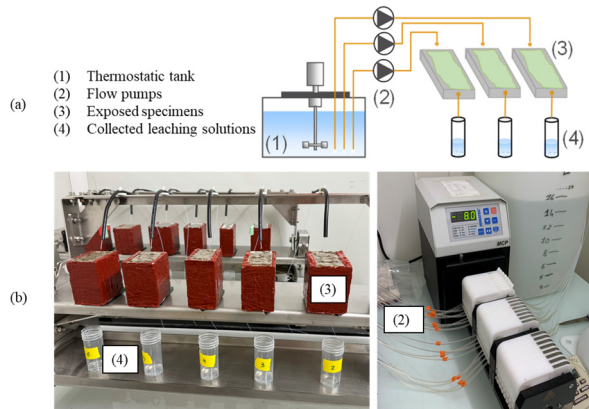


Figure 4. (a) Schematic diagram of the BAC test [19] (b) BAC test setup.

2.6 Analyses of leaching species

During the exposure period, the leaching solution was collected punctually downstream of the exposed specimens (Figure 4). The pH of the collected solutions was measured before they were filtered at $0.2\ \mu\text{m}$ to avoid further biochemical reactions in the tube triggered by microorganisms. The filtered solutions were kept at 4°C until they were analyzed using Inductively Coupled Plasma Optical Emission Spectroscopy (ICP-OES) and High-Performance Ion Chromatography (HPIC) to measure the concentrations of leached calcium and aluminum from the cementitious materials, as well as the sulfate and sulfite produced by the bacterial activity in the biofilm.

To compare the resistance of the exposed specimens to biogenic sulfuric acid, the ratio of the cumulative leached species was standardized based on the initial amount of each component in the material [20]. This was then expressed as a function of the acid produced, obtained from the total quantities of sulfite and sulfate generated, via stoichiometric relations [21].

2.7 Coupled SEM-EDS observations

At the end of each BAC test campaign, coupled microstructural and chemical analyses of the specimens were carried out using scanning electron microscope (SEM) with a JEOL JSM-6380LV microscope on flat sections of the exposed material. The exposed specimens were put into resin (MA2+, O4040, PRESI, Eybens, France) for 24 hours to avoid losing a part of the fragile deteriorated zone in the specimens. They were collected and flat sections were sawn at several centimeters from the outlet edge of the specimens. The polishing of the samples embedded in resin was carried out manually using a series of silicon carbide polishing disks (by Presi) before coating the specimens with a carbon film. The references of the abrasive discs and the sizes of the abrasive particles were: P600– $26\ \mu\text{m}$, P800– $22\ \mu\text{m}$, P1200– $15\ \mu\text{m}$ and P4000– $5\ \mu\text{m}$. The samples were polished with the first disc until the section was flat then progressively with the other

discs. These analyses were coupled with chemical analyses using energy dispersive spectroscopy (XFLASH Series 6130).

3 Results and discussion

The leaching results are presented in Figure 5 for both campaigns of the BAC test noted BAC 1 and BAC 2 respectively in the legend. As previously noted, the first experimental campaign was interrupted at 67 days due to a technical issue, while the second campaign completed the full 3-month exposure period. The graph presents the results corresponding to uncoated substrates, coated uncracked substrates and two coated cracked substrates with different ranges of crack widths. The specimen whose crack width ranges between 150 and $200\ \mu\text{m}$ is referred to in the legend as the narrow cracked and the one between 400 and $500\ \mu\text{m}$ as the wide cracked. In the first campaign, four replicates for coated uncracked specimens and two replicates for uncoated uncracked specimens were tested. Only one replicate was studied for each of the coated narrow and wide cracked specimens. In the second campaign, two replicates were tested for uncracked specimens, and a single replicate for each of the coated narrow and wide cracked specimens.

The different campaigns give consistent results for the same conditions that follow the same trend in both campaigns which gives reliability to the experimental procedure followed. Two significant trends are obtained as a result of presenting the results of different specimens in both campaigns on one curve in Figure 5.

The results of Ca leaching from the specimens exposed to the BAC test are presented in Figure 5 as a function of the quantity of acid produced by the microorganisms, which is calculated based on the quantities of sulfur compounds (sulfate and sulfite) in the collected leaching solution. It is recalled that the leached quantities of Ca from the specimens are represented as standardized leached Ca considering the calcium content of the sound specimens, i.e. Ca content in the CEM III mortar for uncoated specimens and Ca content in the CAC-based material for the coated specimens. These quantities are also standardized to the exposed surface to the biofilm activity. It is consistent to note that the second campaign, which has completed the exposure period of 3 months in the BAC test conditions, reaches much higher quantity of acid of more than $0.07\ \text{mol}$ of H^+ which is about 3 times more than in the first campaign that barely reaches $0.03\ \text{mol}$ of H^+ . This means that the specimens were subject to more aggressive conditions in the second campaign as the exposure period extends so we can observe the results on a longer term.

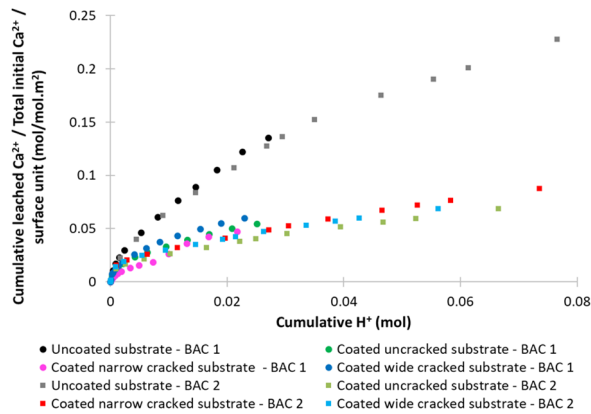


Figure 5. Evolution of standardized cumulative leached Ca^{2+} as function of cumulative produced acid during the exposure to the BAC test in the two campaigns BAC 1 and BAC 2.

In both campaigns, the amount of standardized leached calcium was significantly greater in the case of uncoated specimens whose material is CEM III-based. It reaches values in the order of 3 to 4 times greater than the amount of standardized leached calcium in coated specimens of different properties (cracked or uncracked). Reduced leaching indicates the material's ability to resist the loss of soluble components. This suggests greater chemical and structural stability, essential for withstanding the biogenic acid attack. The performance of the CAC-based coated specimens is consistent with the findings of the literature in the sense of the superior resistance of calcium aluminat cement compared to that of ordinary Portland cement [9,11]. This performance is linked generally to the chemical and microstructural nature of the CAC-based materials especially with the properties of their phases. The stable phases in CAC are aluminium hydroxide (AH_3), which can be stable down to a pH of about 3 or 4, and calcium aluminat hydrates which transform into AH_3 under the acid attack [10,22,23]. This is a key contrast to OPC-based materials which are more vulnerable to biogenic acid attack due to the instability of their calcium-rich phases [24]. The hydrates are mainly calcium aluminat silicat hydrate (C-A-S-H) phases and calcium hydroxid (portlandit) which are thermodynamically unstable at pH values less than 10 and 12.4 respectively and consequently dissolve or decalcify [25]. They react with the acid to form expansive products such as gypsum and ettringit which induce more porosity in the matrix and thus weaken the structure [26,27]. This confirms that the CAC coating is able to protect wastewater treatment structures whose concrete is subject to biodeterioration.

Among the coated specimens, the same leaching trend was followed for the uncracked specimens and cracked ones; whether the crack was of a range between 150 and 200 μm or between 400 and 500 μm . The curves show similar quantities of the leached calcium in the three cases which demonstrates the preservation of the protective function of the coating with the presence of cracks of different ranges of crack width for the specific duration of the test. The reason behind the low influence of the crack on this durability indicator requires investigation in depth for different parameters.

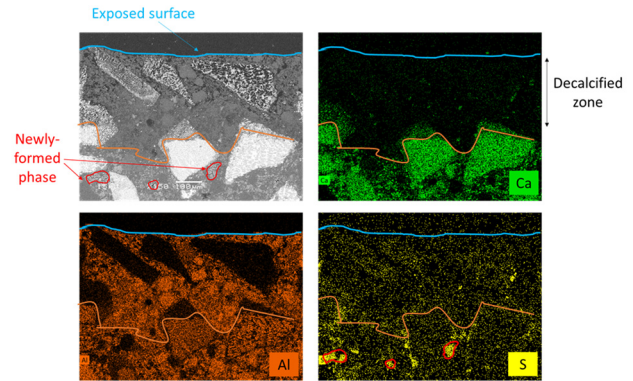


Figure 6. SEM-EDS analyses showing the newly-formed phase close to the exposed surface in the coating of a coated uncracked specimen in the second campaign and the corresponding elemental mappings of the relative distribution of Ca, Al and S.

At the end of the exposure period, coupled SEM-EDS observations were carried out on the exposed materials of both experimental campaigns. Figure 6 presents SEM-EDS analyses showing the newly-formed phase close to the exposed surface and the corresponding elemental mappings of an exposed coated specimen in the second experimental campaign. The deteriorated zone is described as a relatively homogeneous dark grey zone, decalcified and rich in aluminum. It extends from the blue line representing the exposed surface of the specimen until the orange lines traced in Figure 6. In all of the coated specimens in both campaigns, a newly-formed phase, composed of calcium, sulfur and aluminum, was observed close to the exposed surface dispersed at different depths in the first hundreds of micrometers from the surface (Figure 6). This phase is also observed near and in the opening of the crack at about 1 mm from the surface of the cracked coated specimen (150-200 μm) in the first campaign.

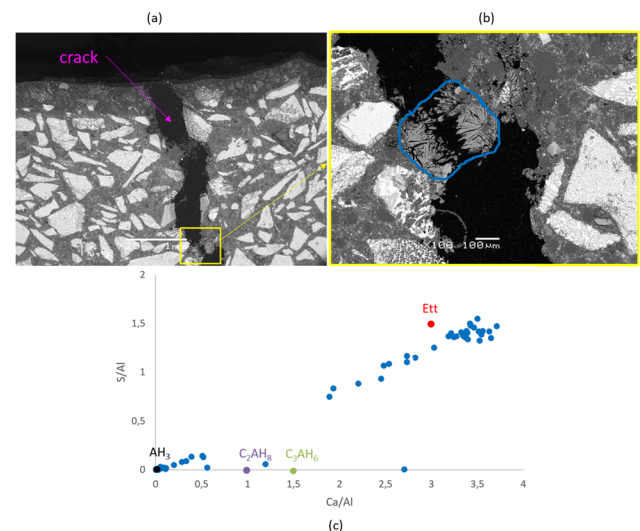


Figure 7. (a)(b) SEM images showing the newly-formed phase close to the crack opening in the wide-cracked coated specimen in BAC 2 (highlighted in blue) in two different magnifications; (c) SEM-EDS analyses of the observed phase in the crack.

EDS analyses suggest it is probably a mix of AH_3 and ettringite phases (Figure 7). A question arises here on the capability of this phase, among possibly other newly-formed phases, to contribute to slowing down the penetration of aggressive agents into the depth of the crack. Although ettringite formation is associated with damage when formed within the cementitious matrix, it may instead contribute positively to crack sealing in this case. This hypothesis arises from the observation that ettringite precipitated within pre-existing crack openings rather than within the dense matrix, suggesting that its growth in unrestrained spaces could promote partial filling of cracks instead of inducing internal stresses and damage.

As a perspective for future work, further microstructural and chemical analyses are planned to understand better the mechanisms and validate the hypotheses concerning the preservation of the coating's protective function in the presence of cracks. Such studies will aim to identify the newly formed or precipitated phases and their spatial distribution relative to the crack opening and exposed surface.

4 Conclusion

To evaluate the efficiency of a calcium aluminate cement-based coating to protect wastewater infrastructures, it is important to understand the effect of cracks emerging from the structure that might propagate into the coating on its protective role. A biological test method, the BAC test, was used to evaluate the effect of the cracks on the performance of the coating. The calcium leaching results of uncracked composite specimens do not show a significant difference when compared to those of cracked composite specimens with different ranges of crack widths (150-200 μm and 400-500 μm). These results demonstrate the capability of the coating to preserve its protective function of the structures in the presence of cracks. Cracks in the range of 150–200 μm are representative of conditions that may occur within acceptable structural limits. While cracks with a width in the range of 400 to 500 μm are structurally unacceptable and would not normally be present in service according to Eurocode limits, they were nevertheless tested to assess the coating's performance under a hypothetical scenario of extensive cracking. Newly-formed phases were observed inside the crack opening and close to it. They possibly have a role in bridging the cracks and slowing down the penetration of aggressive agents which contributes to the ability of the coating to protect the underlying cracked structures. To understand the mechanisms of biodeterioration inside the cracks and improve the understanding of the contributing factors, further microstructural and chemical investigations will be carried on to enable the identification of the observed phases.

Authorship statement (CRediT)

Reem Hoballah: Conceptualization, Investigation, Formal analysis, Validation, Visualization, Writing – Original Draft. **Matthieu Peyre Lavigne:** Resources, Methodology, Formal analysis, Supervision, Writing – Review & Editing. **Cédric Patapy:** Supervision, Writing – Review & Editing.

Laurie Lacarriere: Supervision, Writing – Review & Editing. **Ahmed Toumi:** Supervision, Writing – Review & Editing. **Amr Aboulela:** Formal analysis, Methodology, Supervision. **Alexandra Bertron:** Project administration, Resources, Funding acquisition, Supervision, Writing – Review & Editing.

Acknowledgements

The authors acknowledge Imerys for funding this research and providing the necessary resources to support this work. Their financial support and technical input were essential to the successful completion of the project.

References

- [1] Bartram J, Brocklehurst C, Bradley D, Muller M, Evans B. Policy review of the means of implementation targets and indicators for the sustainable development goal for water and sanitation. *Npj Clean Water* 2018;1:1-5. <https://doi.org/10.1038/s41545-018-0003-0>
- [2] Performance of Cement-Based Materials in Aggressive Aqueous Environments: State-of-the-Art Report, RILEM TC 211 - PAE | SpringerLink n.d. <https://link.springer.com/book/10.1007/978-94-007-5413-3> (accessed December 2, 2024)
- [3] Wells T, Melchers RE, Bond P. Factors involved in the long term corrosion of concrete sewers. 49th Annual Conference of the Australasian Corrosion Association 2009: Corrosion and Prevention 2009 2009.
- [4] Kiliswa MW. Composition and microstructure of concrete mixtures subjected to biogenic acid corrosion and their role in corrosion prediction of concrete outfall sewers. Doctoral Thesis. University of Cape Town, 2016.
- [5] Wu M, Wang T, Wu K, Kan L. Microbiologically induced corrosion of concrete in sewer structures: A review of the mechanisms and phenomena. *Construction and Building Materials* 2020;239:117813. <https://doi.org/10.1016/j.conbuildmat.2019.117813>
- [6] Li X, Jiang G, Grengg C, Mittermayr F. Mechanisms and Processes of Concrete Corrosion in Sewers. In: Jiang G, editor. *Microbiologically Influenced Corrosion of Concrete Sewers: Mechanisms, Measurements, Modelling and Control Strategies*, Cham: Springer International Publishing; 2023, p. 21-34. https://doi.org/10.1007/978-3-031-29941-4_2
- [7] Grengg C, Mittermayr F, Baldermann A, Böttcher ME, Leis A, Koraimann G, et al. Microbiologically induced concrete corrosion: A case study from a combined sewer network. *Cement and Concrete Research* 2015;77:16-25. <https://doi.org/10.1016/j.cemconres.2015.06.011>
- [8] Jiang G, Wightman E, Donose BC, Yuan Z, Bond PL, Keller J. The role of iron in sulfide induced corrosion of sewer concrete. *Water Research* 2014;49:166-74. <https://doi.org/10.1016/j.watres.2013.11.007>
- [9] Herisson J, van Hullebusch ED, Moletta-Denat M, Taquet P, Chaussadent T. Toward an accelerated biodeterioration test to understand the behavior of Portland and calcium aluminate cementitious materials in sewer networks. *International Biodeterioration & Biodegradation* 2013;84:236-43. <https://doi.org/10.1016/j.ibiod.2012.03.007>
- [10] Khan HA, Castel A, Khan MSH, Mahmood AH. Durability of calcium aluminate and sulphate resistant Portland cement based mortars in aggressive sewer environment and sulphuric acid. *Cement and Concrete Research* 2019;124:105852. <https://doi.org/10.1016/j.cemconres.2019.105852>
- [11] Lavigne MP, Bertron A, Botanch C, Auer L, Hernandez-Raquet G, Cockx A, et al. Innovative approach to simulating the biodeterioration of industrial cementitious products in sewer environment. Part II: Validation on CAC and BFSC linings. *Cement and Concrete Research* 2016;79:409-18. <https://doi.org/10.1016/j.cemconres.2015.10.002>
- [12] Grengg C, Mittermayr F, Ukrainczyk N, Koraimann G, Kienesberger S, Dietzel M. Advances in concrete materials for sewer systems affected by microbial induced concrete corrosion: A review. *Water Research* 2018;134:341-52. <https://doi.org/10.1016/j.watres.2018.01.043>

- [13] Aboulela A. Study of the resistance to biodeterioration of innovative low-carbon cementitious materials for application in sewer networks. These de doctorat. Toulouse, INSA, 2022.
- [14] Hoballah R, Peyre Lavigne M, Toumi A, Lacarriere L, Patapy C, Soula C, et al. Durability of Innovative Cementitious Coatings for Concrete Wastewater Treatment Plants: Impact of Cracks on Biodeterioration. In: Beushausen H, Ndawula J, Alexander M, Dehn F, Moyo P, editors. Proceedings of the 7th International Conference on Concrete Repair, Rehabilitation and Retrofitting, Cham: Springer Nature Switzerland; 2025, p. 432-43. https://doi.org/10.1007/978-3-031-75507-1_42
- [15] Fascicule FD P 18-011 : environnements agressifs des bétons armés ou précontraints | Infociments 2014. <https://www.infociments.fr/fascicule-de-documentation-fd-p-19-011> (accessed November 27, 2024)
- [16] Eurocode 2 - NF EN 1992 | Calculs Eurocodes n.d. https://www.calculs-eurocodes.com/eurocode_2 (accessed November 27, 2024)
- [17] Peyre Lavigne M, Bertron A, Auer L, Hernandez-Raquet G, Foussard J-N, Escadeillas G, et al. An innovative approach to reproduce the biodeterioration of industrial cementitious products in a sewer environment. Part I: Test design. Cement and Concrete Research 2015;73:246-56. <https://doi.org/10.1016/j.cemconres.2014.10.025>
- [18] Lavigne MP, Bertron A, Patapy C, Lefebvre X, Paul E. Accelerated test design for biodeterioration of cementitious materials and products in sewer environments. Matériaux & Techniques 2015;103:204. <https://doi.org/10.1051/mattech/2015018>
- [19] Buvignier A, Patapy C, Lavigne MP, Paul E, Bertron A. Resistance to biodeterioration of aluminium-rich binders in sewer network environment: Study of the possible bacteriostatic effect and role of phase reactivity. Cement and Concrete Research 2019; 123:105785. <https://doi.org/10.1016/j.cemconres.2019.105785>
- [20] Aboulela A, Peyre-Lavigne M, Patapy C, Bertron A. Evaluation of the resistance of CAC and BFSC mortars to biodegradation: laboratory test approach. MATEC Web Conf 2018;199:02004. <https://doi.org/10.1051/mateconf/201819902004>
- [21] Aboulela A, Peyre Lavigne M, Buvignier A, Fourré M, Schiettekatte M, Pons T, et al. Laboratory Test to Evaluate the Resistance of Cementitious Materials to Biodeterioration in Sewer Network Conditions. Materials 2021;14:686. <https://doi.org/10.3390/ma14030686>
- [22] Taylor HFW. Cement Chemistry. Thomas Telford; 1997. <https://doi.org/10.1680/cc.25929>
- [23] Scrivener KL, Cabiron J-L, Letourneux R. High-performance concretes from calcium aluminate cements. Cement and Concrete Research 1999;29:1215-23. [https://doi.org/10.1016/S0008-8846\(99\)00103-9](https://doi.org/10.1016/S0008-8846(99)00103-9)
- [24] Grengg C, Ukrainczyk N, Koraimann G, Mueller B, Dietzel M, Mittermayr F. Long-term in situ performance of geopolymer, calcium aluminate and Portland cement-based materials exposed to microbially induced acid corrosion. Cement and Concrete Research 2020;131:106034. <https://doi.org/10.1016/j.cemconres.2020.106034>
- [25] Dauerhaftigkeit von Beton | SpringerLink n.d. <https://link.springer.com/book/10.1007/978-3-642-35278-2> (accessed December 2, 2024)
- [26] Grengg C, Kiliswa M, Mittermayr F, Alexander M. Microbially-induced Concrete Corrosion-A worldwide problem. 2016.
- [27] Cao R, Yang J, Li G, Liu F, Niu M, Wang W. Resistance of the composite cementitious system of ordinary Portland/calcium sulfoaluminate cement to sulfuric acid attack. Construction and Building Materials 2022;329:127171. <https://doi.org/10.1016/j.conbuildmat.2022.127171>